

Fibrous mordenite zeolite - polymer composite adsorbents to methylene blue dye

Kohtaroh Nakamoto, Takaomi Kobayashi

Abstract— Mordenite zeolite - polymer composite fibers prepared by wet - spinning coagulation process were used for removal of methylene blue (MB) dye. The composite fibers had 58.8 wt% loading amount of the mordenite zeolite and were prepared different diameters, when the composite fibers wet-spinneret prepared using 0.3, 0.6 and 0.9 mm needle size in the water coagulation. As tested in adsorption equilibrium of MB at 34, 48 and 48 h of shaking time, the adsorption isotherms of MB for zeolite and the composite fibers were well fitted on Langmuir isotherm models. Notably, it was found that the adsorption ability was significantly enhanced at 10 wt% of polymer concentration, as it was extruded with small size of spinneret diameter, The resultant Langmuir maximum adsorption capacity was 56.8 $\mu\text{mol/g}$ for the composite fiber prepared from 10 wt% of polymer solution with 0.3 mm of spinneret diameter needles.

Index Terms— Mordenite zeolite, fibrous adsorbent, composite adsorbent, methylene blue.

I. INTRODUCTION

Water contamination in wastewater produced from industries has been the serious issue, and for instance, contamination of synthetic dyes has been a one of the problem. Wastewaters containing synthetic dyes are generated from textile industries, photocatalytic industry, coating industry and photochemical application [1] are directly disposed into environment and ecological system was damaged, because of high COD and BOD values [2]. In addition, color of the dyes wastewater is perceived by human eyes, even though dyes concentration is quite low [3]. Also, the colored water reduces light penetration, which interrupts photosynthetic phenomenon for the aquatic bio system [4]. Removal of dyes is taken place by several method such as coagulation method [5], filtration [6], bio degradation [7], photocatalytic degradation [8] and adsorption[9]. Among these treatments, adsorption is entirely effective and straightforward treatment [10]. For the dyes adsorbent, activated carbon commonly has been used due to high surface area providing high adsorption capacities [11-14]. However, activated carbon is costly powder adsorbent, so it is not suitable in the recovery of the adsorbent materials for industrial application [15], after the treatment was finished. Alternatively, zeolite can be a candidate for low cost adsorbent because it naturally occurred and be obtained in abundant amount in volcanogenic marine tuffs [16]. General formula of zeolite is expressed as

Kohtaroh Nakamoto, Department of Materials Science and Technology, Nagaoka University of Technology, Nagaoka, Japan, +81 258478416

Takaomi Kobayashi, Department of Materials Science and Technology, Nagaoka University of Technology, Nagaoka, Japan, +81 258478416

$M_{x/n}[(\text{AlO}_2)_x \cdot (\text{SiO}_2)_y] \cdot z\text{H}_2\text{O}$, where M is cation, n is exchanged cation valency, $x + y$ is the total number of tetrahedra unit and z is number of water molecule [17]. The cation in the zeolite is attracted on constant negative charges on zeolite framework structure, and additionally, the cation is able to be replaced with other cation metals or molecules [18]. Therefore, natural zeolite has been considered for removal of various dyes by some researchers [19, 20]. It was founded that natural zeolite consisted of clinoptilolite, quartz and mordenite has adsorption abilities with Langmuir adsorption capacities of 21.2 and 68.1 $\mu\text{mol/g}$ for rhodamine B and methylene blue [21]. Adsorbent form is important factor to treat stably wastewater. However, powdered zeolite is not sufficient properties for directly applying to contaminated area and column operation. Granule and sphere-shaped zeolites are one of the solution to overcome the drawback, although these shapes decrease the adsorption capacities due to low surface area. In contrast, fibrous adsorbents have a potential for stable treatment without less properties. Young and co-workers fabricated chelating fiber for removal of copper and chromium ions in packed column treatment, the advantages of this fibrous adsorbent are high contact efficiency and low pressure drop in column operation [22]. In our previous work, mordenite zeolite - polyether sulfone composite fiber was fabricated by wet phase inversion technique for decontamination of radioactive cesium and heavy metals in practical treatment [23, 24]. This composite fiber is composed of natural mordenite zeolite particles on porous scaffold of polymer. Especially, it is noted that the adsorption capacities for the composite fiber is not declined even though zeolite is composed on polymer. The purpose of this study is to investigate removability of methylene blue synthetic dye and find optimum preparation condition for the composite fiber.

II. EXPERIMENTAL

A. Reagents

Polyethersulfone (PES, BASF Co. Ltd., Germany) and *N*-Methyl-2-pyrrolidone (NMP, Nacalai Tesque Inc., Japan) were used for preparing polymer solution. Natural zeolite composed of mordenite (Nitto Funka Trading Co. Ltd., Japan.) is washed by NMP before using. Methylene blue (MB, Nacalai Tesque Inc., Japan) was dissolved in distilled water for 1000 mg/L of MB working solution.

B. Preparing mordenite zeolite - polymer composite fibers and their characterization

Mordenite zeolite - polymer composite fibers were prepared by wet - spinning process as mentioned in our previous reports [23]. In the process, composite fiber having

Table 1 Fabrication condition of each composite fibers and properties of zeolite and composite fibers

	Diameter of spinneret (mm)	PES (wt%)	NMP (wt%)	Mordenite zeolite contents in PES (wt%)	Extrusion pressure (MPa)	Diameter (mm)	Tensile strength (MPa)	Apparent volume (cm ³ /g)	BET surface area (m ² /g)
Zeolite	-	-	-	-	-	-	-	-	263
CF-10P-0.9D	0.3	10	90	58.8	0.10	0.91	6.2	0.63	126
CF-10P-0.6D	0.6	10	90	58.8	0.10	0.67	4.8	0.85	143
CF-10P-0.3D	0.9	10	90	58.8	0.10	0.34	2.6	1.04	151
CF-20P-0.3D	0.3	20	80	58.8	0.30	0.29	4.9	0.88	140
CF-30P-0.3D	0.3	30	70	58.8	0.42	0.29	6.4	0.66	144

0.3, 0.6 and 0.9 mm of the wet spinneret diameter needles were used for extrusion of polymer - zeolite solution. The PES content in polymer solution was changed at 10, 20 and 30 wt%, when the amount used of the zeolite was fixed at 58.8 wt% of zeolite content. Extrusion pressures were adjusted at 0.10, 0.30 and 0.42 MPa for the 10, 20 and 30 wt% of polymer solutions including the zeolite respectively, when the 0.3 mm of diameter needle (Table 1). The composite fibers extruded by 0.3, 0.6 and 0.9 mm of diameter were abbreviated as CF-10P-0.3 D, CF-10P-0.6D and CF-10P-0.9D, when 10 wt% of PES concentration was used for the spinning process and when the 20 and 30 wt% dope solutions was used in the 0.3 mm diameter spinneret needle, the fibers were named as CF-20P-0.3D and CF-30P-0.3D, respectively. Table 1 also lists the parameters of fabricating condition for each fibers.

For the characterization of the composite fibers, tensile strength, apparent volume and N₂ adsorption isotherm were measured by following methods. The values of tensile strength were obtained by load measurement device (LTS-500N-S20; Minebea Co. Ltd., Japan). The composite fibers were cut at 5 cm of length for the mechanical measurements, as the fiber was fixed on the grips in the loading device, the crosshead speed was 1.5 mm/s and gauge length were 30 mm in the determination of the tensile strength of the fibers. The tensile strength was obtained by dividing loading force at break point into cross-sectional surface area. The cross-sectional surface area was calculated from the composite fiber diameter which was measured by using micrometer. When you submit your final version, after your paper has been accepted, prepare it in two-column format, including figures and tables.

Apparent volume of the composite fibers was obtained by Archimedes method whose equation is given as

$$V_a = \frac{W_s - W_w}{W_s} \times \frac{1}{(\rho_0 - d)} + \frac{1}{d}$$

where w_s was the dry sample mass (g), w_w was the sample mass in methanol (g), ρ_0 was the density of water (g/cm³), and d is the air density (g/cm³).

For the composite fibers, N₂ adsorption isotherms were measured by nitrogen gas adsorption instrument (Tristar II 3020; Micromeritics Instrument Corp., USA) at -196 °C liquid nitrogen temperature. By using N₂ adsorption results, BET surface area was calculated. The morphology of the composite fibers was examined by scanning electron microscopy (SEM, JSM-5300LVB; JEOL Ltd., Japan) at 15 kV of accelerating voltage.

C. Batch adsorption experiments of MB for the composite fibers

Evaluation of adsorption abilities of MB for each composite fiber was conducted by batch adsorption test as followed. When the composite fibers (0.1g) were placed in 60 mL of polyethylene bottles, 50 mL of MB aqueous solution was added in the different concentration of 15.6, 31.3, 62.5, 125, 188, 250 and 375 μM. These bottles were shaken with a reciprocal shaker at 25 °C for 0.5 - 54 hours. After shaking for certain hours, the liquid was taken to measure these absorbance by ultraviolet-visible spectrophotometer (V-630, JASCO Corp., Japan) at 665 nm. Adsorption test of MB for the mordenite zeolite powder was also carried out to compare the adsorptivity with that of the composite fibers. In the adsorption test, 0.058 g of mordenite zeolite powder was used. Adsorption amount was calculated by following equation,

$$q = \frac{(C_o - C_f) V}{0.01mr}$$

where q was the adsorption amount of heavy metals (μmol/g), m was the mass of adsorbents (g), C_o and C_f were initial and final concentration of the heavy metal solution (μmol/L), respectively, and V was the solution volume (L), r was zeolite content in composite fibers (wt%).

III. RESULTS AND DISCUSSION

A. Characterization of mordenite zeolite - polymer composite fibers having different spinning condition

As shown in Table 1, the resultant values of tensile strength, apparent volume and BET surface area for each composite fiber were listed. The tensile strength of the CF-10P-0.3D, CF-10P-0.6D and CF-10P-0.9D was 2.6, 4.8 and 6.2 MPa and the values of tensile strength were 2.6, 4.9 and 6.4 MPa, respectively. This meant that decreasing polymer concentration resulted in declining strength of the composite fibers. Here, the fiber diameter was almost same in the range of 0.29 - 0.39 mm. The values of apparent volume for the composite fibers were apparently increased with decrease of the PES dope concentration and the fiber diameter. The higher PES concentration and larger diameter size of spinneret needle lead to form dense structure of composite fiber. N₂ isotherm for zeolite and each composite fibers is depicted in Fig. 1. It was not clearly observed that differences of N₂ adsorption isotherms in each composite fiber as seen in Fig. 1. In contrast, as seen in the BET surface area obtained from resultant N₂ adsorption isotherms, CF-10P-0.9D and CF-10P-0.6D showed lower values than that of CF-10P-0.3D. Also, it was seen that increasing values

of BET surface area

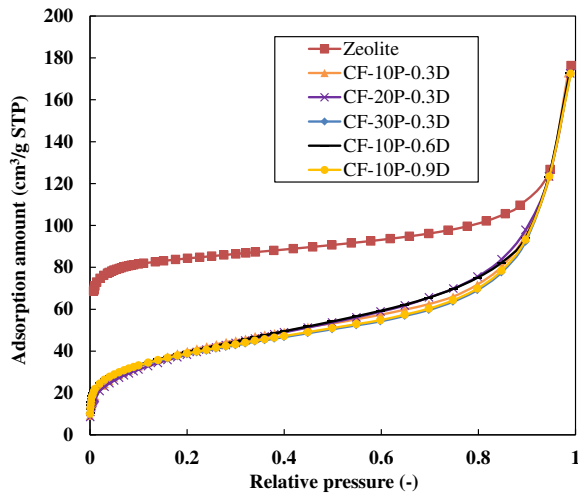


Fig. 1 N₂ adsorption isotherms for zeolite and composite fibers

were range in 126 - 151 m²/g, when with decreasing polymer concentration for the 10, 20 and 30 wt% PES concentration was changed at 58.8 wt% loading of zeolite. Fig. 2 shows SEM images of cross-sectional surface for CF-10P-0.3D, CF-10P-0.6D and CF-10P-0.9D. The diameter apparently became thicker for the composite fibers extruded by thicker needle as seen in the fiber diameter of 0.34, 0.67 and 0.91 mm, respectively (Table 1). It was observed that the zeolite particles were successfully embedded in the PES scaffold for each composite fibers. In the morphology view of the SEM picture, large voids having about 80 μm size were observed for the CF-10P-0.3D, CF-10P-0.6D, but the CF-10P-0.9D has less voids in the cross section view a)-1. As seen in their SEM images for CF-10P-0.3D, CF-20P-0.3D and CF-10P-0.3D (Fig. 2 c), d) and e)), the cross-sectional surface morphology was significantly changed, meaning that the difference in polymer concentration was influenced in the fiber morphology. As noted the finger-like pores were observed in the CF-10P-0.3D, CF-20P-0.3D and CF-30P-0.3D. But the size and number of pores were declined as the PES concentration increased in the dope solution. Especially, it was seen that the CF-10P-0.3D and CF-20P-0.3D had about 3 μm and 1 μm of the finger-like pores, respectively, at the top layer of composite fibers. These morphological differences could be due to coagulation speed of polymer [25]. When the polymer concentration is low and spinneret diameter size is small, coagulation speed of polymer is fast, which causes formation of large size of finger-like pores.

B. Adsorption kinetics and isotherms of MB for mordenite - polymer composite fibers

MB adsorption was investigated for understanding of the adsorption rate and the adsorption equilibrium. The adsorption experiments of zeolite and the composite fibers for MB were conducted in 62.5 μM of initial MB concentration as seen in Fig.3. The time course curves of adsorption amount of MB for zeolite and each composite fibers are depicted in Fig. 3. The adsorption amount of MB rapidly increased within 6 h for zeolite powder. The adsorption equilibrium was confirmed at almost 34 - 50 h for zeolite powder for the

composite fibers. In the case of the composite fibers, it was

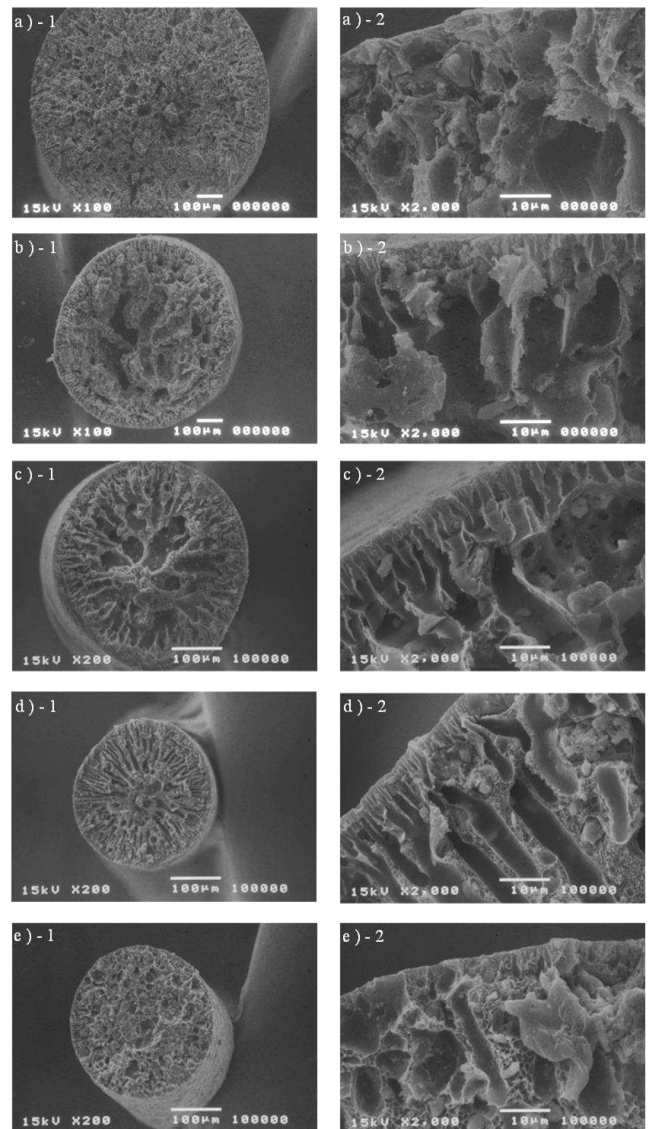


Fig. 2 SEM images of a) CF-10P-0.9D, b) CF-10P-0.6D, c) CF-10P-0.3D, d) CF-20P-0.3D, e) CF-30P-0.3D

seen that adsorption amount of MB slowly increased relative to those of zeolite. For example, the adsorption amounts became constant at 34 h for CF-10P-0.3D and when the values of the CF-10P-0.6D and CF-10P-0.9D at 48h, equilibrium adsorption amounts were 42.3 and 9.16 μmol/g, respectively. These indicated that MB could fastly reached into the limited adsorption sites of zeolite powders in composite fibers. This was because that the PES layer covered the active sites of zeolite. As seen in Fig. 3, the adsorption equilibrium was compared in CF-10P-0.3D, CF-20P-0.3D and CF-30P-0.3D. Interestingly, the equilibrium adsorption amounts were 53.1 and 46.1 μmol/g for CF-10P-0.3D and CF-20P-0.3D. The enhancement of MB adsorption to the CF-10P-0.3D meant that lower dope PES provides efficiently coverage of the zeolite sites in the composite fibers. As seen in Fig. 2, the SEM views suggested this.

Pseudo first-order kinetic and pseudo second-order kinetic were applied to time dependence of adsorption amount of MB for zeolite and composite fibers. Pseudo first order [26] and pseudo second order equations [27] are expressed as following forms, respectively.

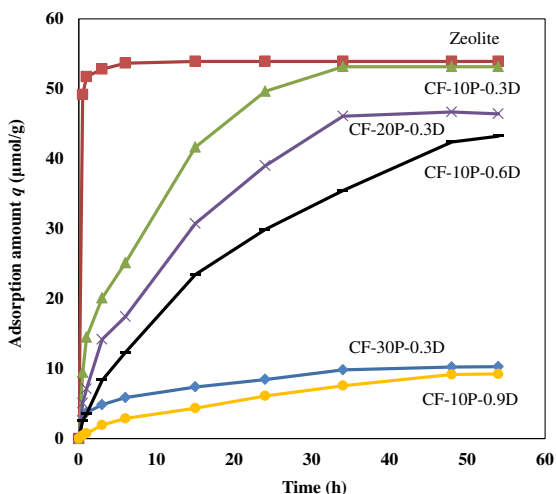


Fig. 3 Time course curve of adsorption amounts of methylene blue

$$\ln q_e - q = \ln q_e - k_1 t$$

where q denote adsorption amount of arsenic ($\mu\text{mol/g}$), q_e present equilibrium adsorption amount of arsenic ($\mu\text{mol/g}$), k_1 is rate constant of pseudo first-order adsorption ($1/\text{h}$). The slope and intercept on plotting $\ln(q_e - q)$ versus t gave the value of k_1 and q_e .

$$\frac{t}{q} = \frac{1}{k_2 q_e^2} + \frac{t}{q_e}$$

where k_2 is rate constant of second-order sorption ($\text{g min}/\mu\text{mol}$). The slope t/q_e and intercept $1/k_2 q_e^2$ give the calculated equilibrium adsorption amount q_e and pseudo second-order adsorption rate constant k_2 . Fig. 4 and 5 show linear plots of pseudo first-order kinetics for zeolite and the composite fibers. Table 2 presents correlation coefficient R^2 and parameters of pseudo first-order and second-order kinetics. The results of Fig. 4 and 5 apparently recognized that the plotting by pseudo second-order kinetic for zeolite and each composite fibers showed well linear relationship in comparison with those of pseudo first-order kinetic. Also, the values of R^2 calculated from pseudo second-order kinetic showed more than 0.95, which indicated that pseudo second-order model could well describe experimental data for zeolite and composite fibers. In the resultant values of adsorption rate constant k_2 , zeolite had the highest values in the experiment systems, as seen, the values for CF-10P-0.9D was higher than those of CF-10P-0.6D and CF-10P-0.3D. Additionally, the values of the CF-10P-0.3D and CF-20P-0.3D were lower than CF-30P-0.3D. This might be because that MB was slowly diffused into the adsorption sites for CF-10P-30D and CF-20P-30D.

Furthermore, adsorption isotherms of MB for zeolite and composite fibers were investigated to know adsorption behavior of MB. For experiment in adsorption isotherm study, adsorption tests were conducted in various initial MB concentrations in the range of 15.6 - 375 μM . The adsorption isotherms of MB for zeolite and each composite fibers are presented in Fig. 6. Interestingly, the CF-10P-0.3D showed comparable behavior with zeolite. The zeolite and composite fibers showed the tendency to become constant values of adsorption amount of MB at certain equilibrium concentrations having 9.2, 44.0, 57.6, 50.0 and 9.5 $\mu\text{mol/g}$ for

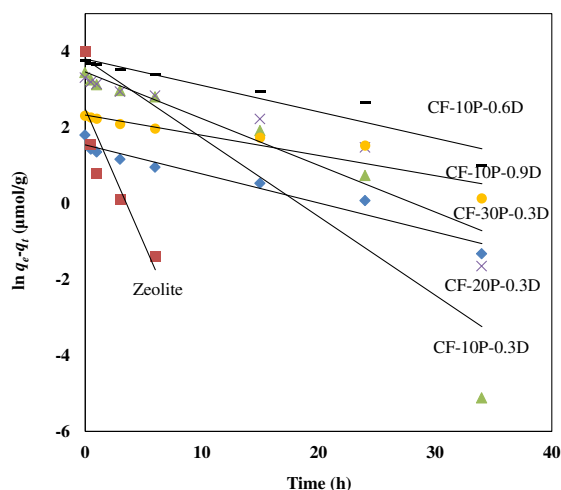


Fig. 4 Pseudo first - order kinetics plots for zeolite and composite fibers

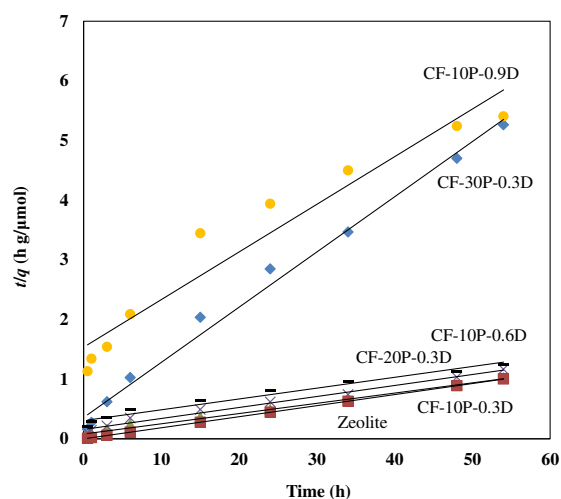


Fig. 5 Pseudo second - order kinetics plots for zeolite and composite fibers

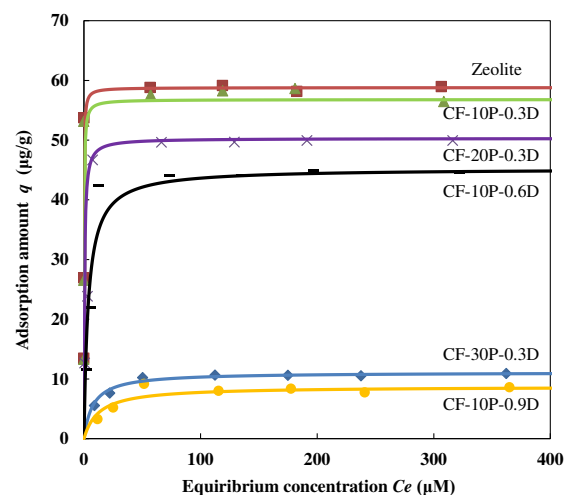


Fig. 6 Adsorption isotherm of MB for zeolite and composite fibers, the initial concentration of MB was 15.6, 31.3, 62.5, 125, 188, 250 and 375 μM

CF-10P-0.3D, CF-10P-0.6D, CF-10P-0.9D, CF-20P-0.3D and CF-30P-0.3D, respectively. These showed that the saturated adsorption amounts increased, as the fiber diameters

Table 2 Parameters of pseudo first and second order kinetics models for zeolite and composite fibers

	Pesudo first order			Pesudo second order		
	q_e ($\mu\text{mol/g}$)	k_1 (1/h)	R^2	q_e ($\mu\text{mol/g}$)	k_2 (g min/ μmol)	R^2
Zeolite	12.0	0.705	0.760	54.1	0.489	1.000
CF-10P-0.9D	10.3	0.053	0.883	12.5	0.042	0.955
CF-10P-0.6D	44.8	0.069	0.914	54.9	0.001	0.971
CF-10P-0.3D	44.6	0.207	0.839	58.5	0.004	0.993
CF-20P-0.3D	32.0	0.123	0.881	54.1	0.002	0.985
CF-30P-0.3D	4.67	0.076	0.941	10.8	0.024	0.991

Table 3 Parameters of Freundlich and Langmuir isotherm models for zeolite and composite fibers

	Freundlich isotherm model			Langmuir isotherm model		
	K_F	$1/n$	R^2	q_m ($\mu\text{mol/g}$)	K_L (L/ μmol)	R^2
Zeolite	38.5	0.083	0.482	58.8	8.50	0.999
CF-10P-0.9D	1.27	0.849	0.670	8.73	0.08	0.993
CF-10P-0.6D	1.26	2.653	0.727	45.2	0.27	0.999
CF-10P-0.3D	2.02	0.088	0.472	56.8	5.68	0.999
CF-20P-0.3D	1.23	0.203	0.762	50.3	2.01	0.999
CF-30P-0.3D	4.33	0.170	0.818	11.1	0.13	0.999

and PES dope concentration decreased. Especially, the CF-10P-0.3D showed high adsorption amount at low equilibrium concentration as seen similarly in that of zeolite. To investigate more the adsorption behavior of the MB for the zeolite and composite fibers, two isotherm models of Freundlich and Langmuir models were applied to their experimental adsorption isotherm data. It is known that Freundlich isotherm model are empirical model for describing multi-layer adsorption or adsorption on inhomogeneous adsorption sites. The equation are expressed as

$$q_e = K_F C_e^{\frac{1}{n}}$$

where q_e is the equilibrium adsorption amount ($\mu\text{mol/g}$), K_F and n are Freundlich constants (-), and C_e denotes equilibrium concentration ($\mu\text{mol/g}$). This equation can be deformed as following liner form equation

$$\ln q_e = \ln K_F + \frac{1}{n} \ln C_e$$

Thus, Freundlich constants K_F and n can be calculated from the slope and intercept on plotting $\ln q_e$ versus $\ln C_e$. On the other hand, Langmuir isotherm model is theoretical model, which are well fitted on monolayer adsorption system [28, 29]. This is presented by following equation

$$q = \frac{q_m K_L C_e}{1 + K_L C_e}$$

as equation deformed to linear formula of

$$\frac{C_e}{q_e} = \frac{C_e}{q_m} + \frac{1}{q_m K_L}$$

Here, q_e denotes equilibrium adsorption amount (μM), K_L presents the Langmuir constant (L/ μmol), and q_m is maximum adsorption capacity ($\mu\text{mol/g}$). The slope and intercept of linear approximation on plotting C_e/q_e versus C_e could provide q_m and K_L . The reasonability of two models for experimental data are decided from values of correlation coefficient R^2 of linear approximation. The resultant values of parameters and R^2 of two models are listed in Table 3. Figs. 7 and 8 show Freundlich isotherm and Langmuir isotherm linear plots for zeolite and composite fibers. The values of R^2

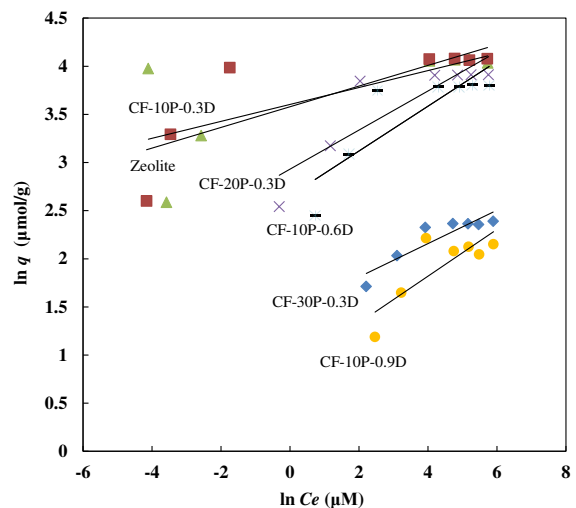


Fig. 7 Freundlich adsorption isotherm plots of MB for zeolite and composite fibers

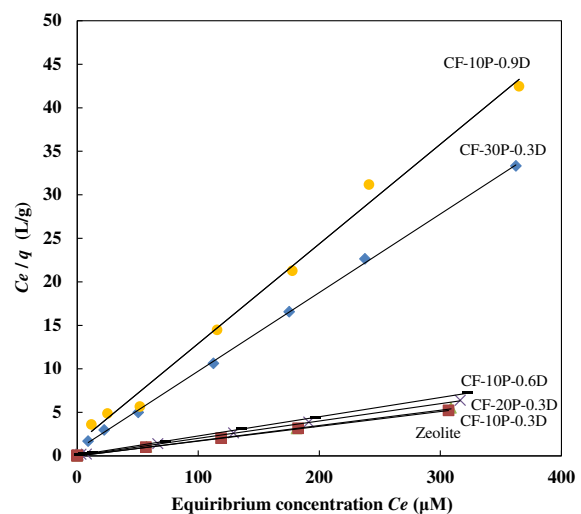


Fig. 8 Langmuir adsorption isotherm plots of MB for zeolite and composite fibers

obtained in the Langmuir isotherm model meant that significant fitting to the present results were observed relative to Freundlich isotherm model. As presented in Fig. 8, the Langmuir isotherm linear plots clearly showed linear relationship for zeolite and composite fibers. Thus, MB could be absorbed on both zeolite and composite fibers in monolayer adsorption system. In the maximum adsorption capacities and Langmuir constant, these values for CF-10P-0.9D and CF-30P-0.3D were notably low in comparison with zeolite, and other composite fibers.

IV. CONCLUSION

The mordenite zeolite - polymer composite fibers were fabricated by wet - spinning process in various preparation conditions and then were used for MB adsorption test. The time dependence of the adsorption amounts of MB showed that CF-10P-0.3D prepared with 10 wt% of the PES dope concentration and 0.3 mm size of spinneret diameter was effective adsorptivity as well as that of zeolite. The adsorption kinetics were obeyed to pseudo second - order model and adsorption isotherms of MB revealed Langmuir adsorption isotherm model.

ACKNOWLEDGMENT

The authors would like to thank the Kasai corporation for the support of this study.

REFERENCES

[1] S. Sohrabnezhad, A. Pourahmad, Comparison absorption of new methylene blue dye in zeolite and nanocrystal zeolite, *Desalination*, 256 (2010) 84-89.

[2] S.M. Burkinshaw, G. Salihu, The role of auxiliaries in the immersion dyeing of textile fibres: Part 1 an overview, *Dyes and Pigments*, (2017).

[3] M.A. Fahim Bin AbdurRahman, M. Zainal Abedin, Dyes Removal From Textile Wastewater Using Orange Peels, *International Journal of Scientific & Technology Research*, 2 (2013) 47-50.

[4] M. Arami, N.Y. Limaee, N.M. Mahmoodi, N.S. Tabrizi, Removal of dyes from colored textile wastewater by orange peel adsorbent: Equilibrium and kinetic studies, *Journal of Colloid and Interface Science*, 288 (2005) 371-376.

[5] C.Y. Teh, P.M. Budiman, K.P.Y. Shak, T.Y. Wu, Recent Advancement of Coagulation–Flocculation and Its Application in Wastewater Treatment, *Industrial & Engineering Chemistry Research*, 55 (2016) 4363-4389.

[6] B. Van der Bruggen, I. De Vreese, C. Vandecasteele, Water Reclamation in the Textile Industry: Nanofiltration of Dye Baths for Wool Dyeing, *Industrial & Engineering Chemistry Research*, 40 (2001) 3973-3978.

[7] S.K. Sen, S. Raut, P. Bandyopadhyay, S. Raut, Fungal decolouration and degradation of azo dyes: A review, *Fungal Biology Reviews*, 30 (2016) 112-133.

[8] G. Zayani, L. Bousselemi, F. Mhenni, A. Ghrabi, Solar photocatalytic degradation of commercial textile azo dyes: Performance of pilot plant scale thin film fixed-bed reactor, *Desalination*, 246 (2009) 344-352.

[9] A. Martins, N. Nunes, Adsorption of a Textile Dye on Commercial Activated Carbon: A Simple Experiment To Explore the Role of Surface Chemistry and Ionic Strength, *Journal of Chemical Education*, 92 (2015) 143-147.

[10] K.B. Tan, M. Vakili, B.A. Horri, P.E. Poh, A.Z. Abdullah, B. Salamatinia, Adsorption of dyes by nanomaterials: Recent developments and adsorption mechanisms, *Separation and Purification Technology*, 150 (2015) 229-242.

[11] M. Goswami, P. Phukan, Enhanced adsorption of cationic dyes using sulfonic acid modified activated carbon, *Journal of Environmental Chemical Engineering*, 5 (2017) 3508-3517.

[12] M.J. Iqbal, M.N. Ashiq, Adsorption of dyes from aqueous solutions on activated charcoal, *Journal of Hazardous Materials*, 139 (2007) 57-66.

[13] V. Gómez, M.S. Larrechi, M.P. Callao, Kinetic and adsorption study of acid dye removal using activated carbon, *Chemosphere*, 69 (2007)

1151-1158.

[14] S. Preethi, A. Sivasamy, S. Sivanesan, V. Ramamurthi, G. Swaminathan, Removal of Safranin Basic Dye from Aqueous Solutions by Adsorption onto Corncob Activated Carbon, *Industrial & Engineering Chemistry Research*, 45 (2006) 7627-7632.

[15] F. Bouaziz, M. Koubaa, F. Kallel, R.E. Ghorbel, S.E. Chaabouni, Adsorptive removal of malachite green from aqueous solutions by almond gum: Kinetic study and equilibrium isotherms, *International Journal of Biological Macromolecules*, (2017).

[16] P. Cappelletti, A. Colella, A. Langella, M. Mercurio, L. Catalanotti, V. Monetti, B. de Gennaro, Use of surface modified natural zeolite (SMNZ) in pharmaceutical preparations Part I. Mineralogical and technological characterization of some industrial zeolite-rich rocks, *Microporous and Mesoporous Materials*, 250 (2017) 232-244.

[17] P.K. Bajpai, M.S. Rao, K.V.G.K. Gokhale, Synthesis of Mordenite Type Zeolites, *Industrial & Engineering Chemistry Product Research and Development*, 17 (1978) 223-227.

[18] Y. Zhan, H. Zhang, J. Lin, Z. Zhang, J. Gao, Role of zeolite's exchangeable cations in phosphate adsorption onto zirconium-modified zeolite, *Journal of Molecular Liquids*, 243 (2017) 624-637.

[19] I. Humelnicu, A. Băiceanu, M.-E. Ignat, V. Dulman, The removal of Basic Blue 41 textile dye from aqueous solution by adsorption onto natural zeolitic tuff: Kinetics and thermodynamics, *Process Safety and Environmental Protection*, 105 (2017) 274-287.

[20] V. Meshko, L. Markovska, M. Mincheva, A.E. Rodrigues, Adsorption of basic dyes on granular activated carbon and natural zeolite, *Water Research*, 35 (2001) 3357-3366.

[21] S. Wang, Z.H. Zhu, Characterisation and environmental application of an Australian natural zeolite for basic dye removal from aqueous solution, *Journal of Hazardous Materials*, 136 (2006) 946-952.

[22] Y.G. Ko, Y.J. Chun, C.H. Kim, U.S. Choi, Removal of Cu(II) and Cr(VI) ions from aqueous solution using chelating fiber packed column: Equilibrium and kinetic studies, *Journal of Hazardous Materials*, 194 (2011) 92-99.

[23] T. Kobayashi, M. Ohshiro, K. Nakamoto, S. Uchida, Decontamination of Extra-Diluted Radioactive Cesium in Fukushima Water Using Zeolite–Polymer Composite Fibers, *Industrial & Engineering Chemistry Research*, 55 (2016) 6996-7002.

[24] K. Nakamoto, M. Ohshiro, T. Kobayashi, Mordenite zeolite–Polyethersulfone composite fibers developed for decontamination of heavy metal ions, *Journal of Environmental Chemical Engineering*, 5 (2017) 513-525.

[25] Z.-L. Xu, F. Alsahy Qusay, Polyethersulfone (PES) hollow fiber ultrafiltration membranes prepared by PES/non-solvent/NMP solution, *Journal of Membrane Science*, 233 (2004) 101-111.

[26] E. Tümay Özer, B. Osman, A. Kara, N. Beşirli, Ş. Gücer, H. Sözeri, Removal of diethyl phthalate from aqueous phase using magnetic poly(EGDMA–VP) beads, *Journal of Hazardous Materials*, 229-230 (2012) 20-28.

[27] Y. Liu, New insights into pseudo-second-order kinetic equation for adsorption, *Colloids and Surfaces A: Physicochemical and Engineering Aspects*, 320 (2008) 275-278.

[28] I. Langmuir, THE CONSTITUTION AND FUNDAMENTAL PROPERTIES OF SOLIDS AND LIQUIDS. PART I. SOLIDS, *Journal of the American Chemical Society*, 38 (1916) 2221-2295.

[29] E. Worch, Adsorption technology in water treatment Fundamentals, processe, and modeling, Gruyter, Germany, 2012.